

**Kenneth J. H. Phillips, Uri Feldman  
and Enrico Landi**

Ultraviolet and X-ray  
Spectroscopy of the  
Solar Atmosphere

CAMBRIDGE UNIVERSITY PRESS

Cambridge, New York, Melbourne, Madrid, Cape Town, Singapore, São Paulo, Delhi

Cambridge University Press

The Edinburgh Building, Cambridge CB2 8RU, UK

Published in the United States of America by Cambridge University Press, New York

[www.cambridge.org](http://www.cambridge.org)

Information on this title: [www.cambridge.org/9780521841603](http://www.cambridge.org/9780521841603)

© K. J. H. Phillips, U. Feldman and E. Landi 2008

This publication is in copyright. Subject to statutory exception and to the provisions of relevant collective licensing agreements, no reproduction of any part may take place without the written permission of Cambridge University Press.

First published 2008

Printed in the United Kingdom at the University Press, Cambridge

*A catalogue record for this publication is available from the British Library*

*Library of Congress Cataloging-in-Publication Data*

Phillips, Kenneth J. H.

Ultraviolet and x-ray spectroscopy of the solar atmosphere / Kenneth J. H. Phillips, Uri Feldman, Enrico Landi.

p. cm. — (Cambridge astrophysics series)

Includes bibliographical references and index.

ISBN 978-0-521-84160-3

1. Spectrum, Solar. 2. Ultraviolet spectroscopy. 3. X-ray spectroscopy.

I. Feldman, U. II. Landi, Enrico. III. Title.

QC455.P55 2008

523.7—dc22

2008008434

ISBN 978-0-521-84160-3 hardback

Cambridge University Press has no responsibility for the persistence or accuracy of URLs for external or third-party internet websites referred to in this publication, and does not guarantee that any content on such websites is, or will remain, accurate or appropriate.

---

# Contents

---

<i>Preface</i>	<i>page 4</i>
<b>1 The solar atmosphere</b>	<b>7</b>
1.1 Introduction	7
1.2 Chromosphere, Transition Region, and Corona	8
1.3 The Ultraviolet and X-ray Spectrum of the Solar Atmosphere	10
1.4 Structure of the Solar Atmosphere	15
1.5 Dynamics of the Solar Atmosphere	20
1.6 The Active Sun	22
1.7 Physical Conditions and Energy Balance	26
1.8 Ionization and Excitation Conditions	30
1.9 Chemical Composition	32
1.10 Solar-type Stars	34
<b>2 Fundamentals of solar radiation</b>	<b>37</b>
2.1 Wavelength ranges	37
2.2 Specific Intensity and Flux	38
2.3 Radiative transfer and the source function	40
2.4 Radiation from the Solar Atmosphere	41
2.5 Radiant Intensity and Flux	46
<b>3 Fundamentals of atomic physics</b>	<b>51</b>
3.1 Introduction	51
3.2 The one-electron atom - Bohr's theory	51
3.3 The one-electron atom: Quantum theory	55
3.4 The multi-electron atom: Quantum theory	60
3.5 Isoelectronic sequences	69
3.6 Interaction between atoms and electromagnetic fields	70
3.7 Atomic codes	81
<b>4 Mechanisms of formation of the solar spectrum</b>	<b>83</b>
4.1 Introduction	83
4.2 Collisional excitation and de-excitation of atomic levels	83
4.3 Level populations	88

<b>2</b>	<b><i>Contents</i></b>	
4.4	Ionization and recombination	94
4.5	Ion populations and ionization equilibrium	101
4.6	Line radiation	103
4.7	Continuum radiation	106
4.8	Spectral line profiles	117
4.9	Other excitation mechanisms of spectral lines	120
4.10	X-ray Fluorescence Lines in Flares	121
	<b>5 Plasma diagnostic techniques</b>	<b>130</b>
5.1	Introduction	130
5.2	Electron density diagnostics	130
5.3	Electron temperature diagnostics	142
5.4	Ion temperature diagnostics	151
5.5	Emission measure diagnostics	154
5.6	Differential emission measure diagnostics	156
5.7	Element abundance diagnostics	162
5.8	Ion abundances	166
5.9	Plasma dynamics diagnostics	167
5.10	Magnetic field diagnostics	173
5.11	Spectral codes for solar corona research	175
	<b>6 Ultraviolet and X-ray emission lines</b>	<b>177</b>
6.1	The 1–7 Å Range	178
6.2	The 7–23 Å Range	180
6.3	The 23–170 Å Range	181
6.4	The 170–630 Å Range	184
6.5	The 630–2000 Å Range (off-limb spectrum)	187
6.6	The 630–2000 Å Range (disk spectrum)	192
	<b>7 Spectrometers and Imagers for observing the Solar Ultraviolet and X-ray Spectrum</b>	<b>198</b>
7.1	Introduction	198
7.2	Transmittance properties of materials	199
7.3	Reflectance of VUV, EUV, and X-ray radiation from Materials	200
7.4	Ultraviolet Spectrometers	203
7.5	X-ray spectrometers	210
7.6	Imaging instruments	216
7.7	Instrument calibration	220
7.8	Summary of spacecraft instruments	223
	<b>8 Quiet Sun and coronal holes</b>	<b>225</b>
8.1	Introduction	225
8.2	Quiet Sun corona and coronal holes: structure	226
8.3	Quiet Sun corona and coronal holes: plasma properties	229
8.4	Quiet Sun transition region	234
8.5	Nonthermal broadening of ultraviolet emission lines	237

<b><i>Contents</i></b>	<b>3</b>
8.6 Quiet Sun Dynamic Phenomena	239
8.7 Coronal waves and oscillations	244
<b>9 Active regions</b>	<b>247</b>
9.1 Introduction	247
9.2 Structure of active regions	248
9.3 Active region loops	252
9.4 Active region densities	257
9.5 Active region transient phenomena	258
<b>10 Solar Flares</b>	<b>271</b>
10.1 Introduction	271
10.2 X-ray Flare Spectra	271
10.3 Ultraviolet Flare Spectra	276
10.4 Flare Temperatures and Emission Measures	277
10.5 Flare Densities	282
10.6 Flare Morphology	284
10.7 Mass Motions in Flares	287
10.8 Nonthermal Electrons	289
10.9 X-ray Fluorescence Lines in Flares	289
10.10 Ionization Equilibrium in Flares	290
10.11 <i>GOES</i> Observations of Flares	291
<b>11 Element abundances</b>	<b>308</b>
11.1 Introduction	308
11.2 Solar wind abundances	311
11.3 Abundances in quiet Sun and coronal hole regions	312
11.4 FIP bias in distinct solar structures	316
11.5 The FIP bias rate of change in the solar atmosphere	318
11.6 Is the FIP bias magnitude FIP-dependent?	320
11.7 The number of free electrons in the photosphere	321
11.8 Summary	323
<i>Appendices</i>	325
11.9 Appendix 1: Units	325
11.10 Appendix 2: Further reading	326
<i>Glossary of terms</i>	328
<i>Appendix: Line List 1</i>	340
<i>Appendix: Line List 2</i>	367
<i>Appendix: Line List References</i>	371
<i>References</i>	373
References	373
<i>Index</i>	385

---

# Preface

---

Even those not engaged in solar physics will have noticed a huge increase in space observations of the solar atmosphere over the past few years. The last ten years especially have seen several notable space missions launched by NASA, the European Space Agency (ESA), the Japanese and Russian space agencies, and several other organizations, among which have been the *Yohkoh* and *RHESSI* X-ray spacecraft, *SOHO*, *TRACE*, and *CORONAS-F* which have on board high-resolution instruments working in the extreme ultraviolet spectrum, and most recently the *STEREO* and *Hinode* missions, both launched in late 2006, all of which are making spectacular observations in the visible, ultraviolet, and soft X-ray regions. Major contributions to our knowledge have also been made by rocket-borne instruments such as SERTS and EUNIS, working in the extreme ultraviolet.

The increase in our understanding of the solar atmosphere giving rise to this emission has been enormous as a direct result of studying the data from these instruments. We have built on the knowledge gained from previous large solar missions such as the *Skylab* mission and *Solar Maximum Mission* to develop models for the solar atmosphere and for phenomena such as flares and coronal mass ejections. However, to the dismay of some but the excitement of most, we are now presented with a picture of the solar atmosphere that is far more dynamic and complex than we ever expected from early spacecraft or ground-based telescopes. Consequently, it has really been the case that as fast as we solve some problems, others are created that will obviously need great ingenuity in finding satisfactory physical explanations. A case in point is the ever-elusive coronal heating problem, one that has been with us ever since the mega-kelvin temperatures of the solar corona were discovered, from optical spectroscopy, in the 1940s.

Much of our knowledge has come from studying images of phenomena, monochromatic or in broad-band ranges. But quantitative work, just as with studies of stars, begins with spectroscopic studies. Ultraviolet and X-ray spectra give us information about temperatures, densities, flow velocities, filling factors (indicating to what extent we are spatially resolving features), emission measures.

Ultraviolet and X-ray spectra give us information about temperatures, densities, flow velocities, filling factors (indicating to what extent features are being spatially resolved), thermal structure, element abundances, ionization state of solar plasmas in the outer parts of the solar atmosphere: the chromosphere, the corona and the

enigmatic transition region. They also allow insight into all phenomena in the solar atmosphere, e.g. flares, jets, and prominences.

Though there have been review articles and portions of textbooks devoted to solar spectroscopy in the ultraviolet and X-ray region, no monograph has yet been written that specifically addresses this aspect. This book is meant to fill this gap in the literature. First, we review basic concepts in studies of the solar atmosphere, with descriptions of the properties of the various parts of the solar atmosphere and phenomena (Chapter 1). Then basic concepts in radiation from the solar atmosphere, from the photosphere outwards, are given, with applications specific to UV and X-ray spectroscopy (Chapter 2). Basic atomic theory, needed in understanding spectral line and continuum formation and interpretation, is given in Chapter 3, with descriptions of how lines and continua are formed (Chapter 4). We expect these two chapters to be most useful for students, post-graduates and others who wish to have an understanding of atomic physics and how it relates to spectroscopy. How narrow-band images and spectral line ratios particularly are used in 'diagnosing' parts of the solar atmosphere, i.e. finding densities, temperatures, and other parameters, is dealt with in Chapter 5, including specific examples of lines that are suitable for diagnostic purposes (Chapter 6). A description of current and recent instrumentation is given in Chapter 7. Later chapters (8, 9, 10) review recent literature giving applications of spectroscopic techniques in the UV and X-ray bands to the quiet and active Sun and the particular case of solar flares. As the literature is now so extensive, this review has necessarily been subjective and has quite likely omitted work that others will consider important. We apologize to any who feel that their work is not justly treated in these chapters.

One of the most significant findings using ultraviolet and X-ray spectroscopy in recent years has been the discovery of departures of element abundances in the solar atmosphere from those in the solar photosphere, with a clear link with the first ionization potential (FIP) of these elements. This result first became clear in the study of solar wind and solar energetic particles, but spectroscopically determined abundances showed that this was true for the solar corona and maybe other parts of the solar atmosphere. A more personal view on this topic is given in Chapter 11, with additional evidence that is not yet in the published literature.

Notes on units (following the still current usage in solar physics, we use the c.g.s. system), a glossary, and list of emission lines in the solar ultraviolet and soft X-ray spectrum are also given.

We are grateful to the many colleagues who have helped us in the task of writing this book. We thank those who have allowed us to use figures and other results from their published works; their names are acknowledged in figure captions. Data from many spacecraft missions are freely available from web-based sources, and we have taken advantage of obtaining images and spectra accordingly. We particularly acknowledge teams of scientists who have made these data sources available to us and to the solar community generally. We are also particularly indebted to colleagues who offered their time to read portions of the book manuscript, and who have helped enormously by making very helpful suggestions or correcting our misconceptions. They are: A. K. Bhatia, J. L. Culhane, J. M. Laming, M. Landini, J. C. Raymond. We are grateful to our institutes, Mullard Space Science Laboratory (University

## **6**      *Preface*

College London) and Naval Research Laboratory (the US Department of the Navy) for their support during the writing of this book.

# 1

---

## The solar atmosphere

Kenneth J.H. Phillips, Uri Feldman, & Enrico Landi

---

### 1.1 Introduction

The solar atmosphere may be broadly defined as that part of the Sun extending outwards from a level known as the photosphere where energy generated at the Sun's core begins to escape into space as radiation. Regions progressively deeper than this level are characterized by increasing densities where there are continual interactions between atoms or ions and radiation. None of this radiation escapes into space. Such regions constitute the solar interior. The photosphere can loosely be regarded as the Sun's surface, though more precisely it is a thin layer. The base of the photosphere depends on the wavelength of the radiation. A common but arbitrary definition is where the *optical depth*  $\tau$ , i.e. the integral of the absorption coefficient over path-length, is unity for radiation of wavelength 5000 Å (corresponding to the green part of the visible spectrum), written  $\tau_{5000} = 1$ . We shall give further definitions of these concepts in Chapter 2. The temperature of the  $\tau_{5000} = 1$  level is approximately 6400 K. Much of the absorption of visible and infrared radiation, which makes up the bulk of the Sun's radiant energy escaping from the photosphere, is due to the negative hydrogen ion  $H^-$ . The absorption of photons of radiation  $h\nu$  occurs by reactions like  $h\nu + H^- \rightarrow H + e^-$ , i.e. the break-up of the  $H^-$  ion to form a hydrogen atom and free electron. At sufficiently high densities, the reverse reaction ensures the replenishment of  $H^-$  ions. The rapid fall-off of total density proceeding outwards from the Sun leads to a depletion of  $H^-$  ions, and thus a decrease in absorption coefficient and optical depth. The consequence of this is that the Sun appears to have a very sharp edge at optical wavelengths.

Energy is generated in the Sun's core by nuclear reactions, in particular fusion of four protons to form  ${}^4\text{He}$  nuclei. The energy is transferred to the rest of the solar interior by radiation out to  $0.667R_\odot$  where  $R_\odot = 696,000$  km is the solar radius, i.e. radius of the photosphere, and by convection from  $0.667R_\odot$  to the photosphere. By the First Law of Thermodynamics, the temperature continuously falls with distance from the energy-generating region at the Sun's core. This fall-off of temperature would be expected to continue in the solar atmosphere, starting from the base of the photosphere where  $\tau_{5000} = 1$ . In fact the temperature rises, eventually reaching extremely large values, giving rise to an atmosphere which emits radiation at extreme ultraviolet and X-ray wavelengths. The nature of this emission, and what can be learned from it, are the subject matter of this book.

## 1.2 Chromosphere, Transition Region, and Corona

Model solar atmospheres are a guide to the way in which temperature varies with height and help to provide definitions of atmospheric regions. In the well-known VAL models (Vernazza et al. (1981)), an initial temperature *vs.* height plot is used to calculate using radiative transfer equations the emergent spectrum which is then compared with observed spectra, and adjustments to the initial temperature distribution made. According to their Model C (average solar atmosphere), there is a fall-off of temperature from the  $\tau_{5000} = 1$  level, reaching  $\sim 4400$  K at a height of about 500 km above  $\tau_{5000} = 1$ , the temperature minimum level. Above the temperature minimum, the temperature rises to form a broad plateau at  $\sim 6000$  K, over a height range of approximately 1000–2000 km, then rises sharply. To account for large radiation losses due to hydrogen Ly- $\alpha$  emission, the VAL models require a small plateau at  $\sim 20\,000$  K on the sharp temperature rise. According to the model by Gabriel (1976), this rise continues on to temperatures of  $1.4 \times 10^6$  K or more. For many authors, the solar *chromosphere* is defined to be the region from the temperature minimum up to where the temperature is approximately  $\sim 20\,000$  K. The region of the solar atmosphere where the temperature reaches  $\sim 10^6$  K and where the densities are very low compared with the chromosphere is the solar *corona*. A further region having temperatures of  $\sim 10^5$  K known as the *transition region* is in solar atmospheric models a thin layer separating the dense, cool chromosphere and tenuous, hot corona. Figure 1.1 shows (solid curve) the variation of temperature in the lower part of the solar atmosphere (heights up to 30 000 km above the  $\tau_{5000} = 1$  level), together with variations in the number densities ( $\text{cm}^{-3}$ ) of neutral hydrogen ( $N_H$ ) and free electrons ( $N_e$ ), according to three quiet-Sun models (Vernazza et al. (1981); Fontenla et al. (1990); Gabriel (1976)) which have been patched together over appropriate height ranges. Further details are given in Section 1.7 and Table 1.1.

The solar chromosphere is observable in visible wavelengths by forming images, known as spectroheliograms, in narrow wavelength bands around the cores of certain absorption or Fraunhofer lines that have their origins in the lower chromosphere. These include the hydrogen Balmer- $\alpha$  (or H $\alpha$ ) line at 6563 Å (red part of spectrum) and singly ionized calcium (Ca II) H and K lines at 3968 Å and 3933 Å (blue) respectively. also has a visible-wavelength emission-line spectrum which is apparent at the beginning and end of the totality phase of total solar eclipses, when the Moon passes in front of the photosphere, covering up its intensely bright radiation. It is then clear that the chromosphere's extent is far greater than the 2000 km predicted by solar models and indeed its nature is far from being a uniform layer of the atmosphere. Rather, extending out from about 2000 km up to  $\sim 10\,000$  km are transient pencil-shaped structures called spicules. In H $\alpha$  spectroheliograms, they are dark features on the disk covering about 10% of the solar surface. Further, the white-light corona seen during total eclipses is observed to be highly non-uniform, consisting of streamers and loops that stretch out hundreds of thousands of km above the limb. The white-light emission arises from the Thomson scattering of photospheric light by the fast-moving free electrons in the high-temperature corona. Observations, therefore, show that model atmospheres, while useful in describing the way in which temperature rises (and density decreases) with height, have limitations in that the high degree of structure in the chromosphere and corona is not properly reproduced. The nature of

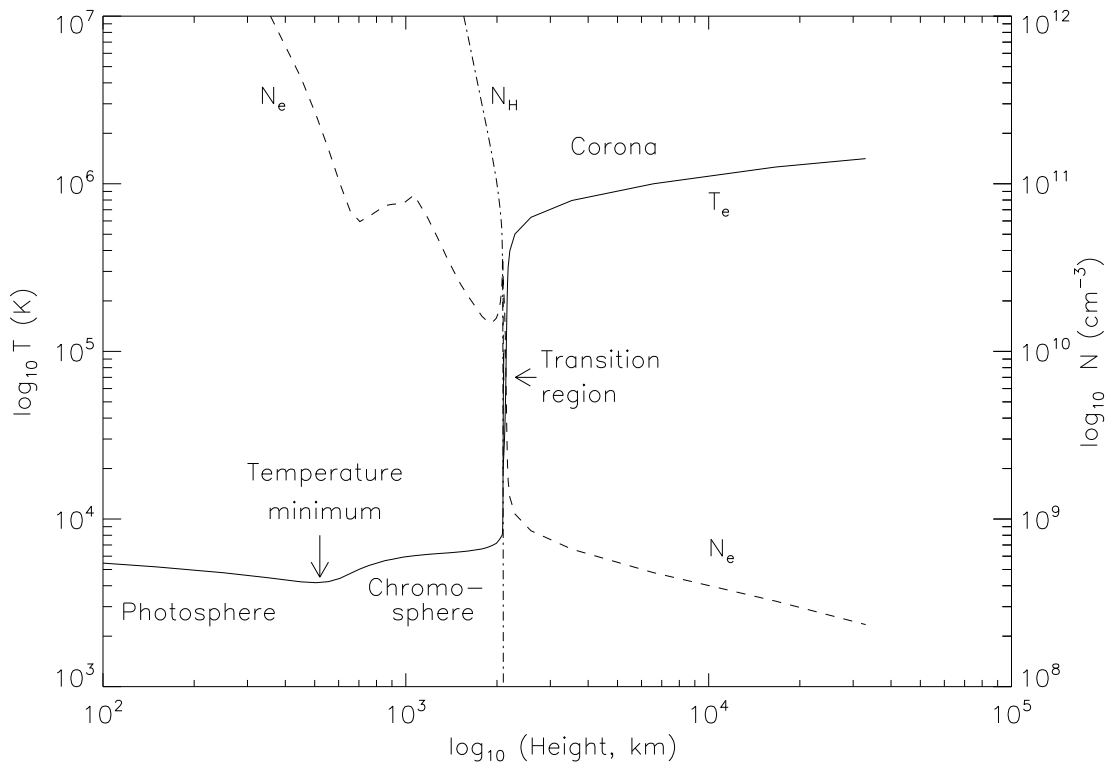


Fig. 1.1. The variation of temperature with height in the solar atmosphere (solid curve), based on one-dimensional model calculations of Vernazza et al. (1981), Fontenla et al. (1988), and Gabriel (1976). The chromospheric and transition region part of this model atmosphere is for the average quiet Sun. Based on these idealized representations of the solar atmosphere, the transition region is a thin layer with  $T = 10^5$  K separating the chromosphere and corona. Variations in the number densities ( $\text{cm}^{-3}$ ) of neutral hydrogen atoms ( $N_H$ ) and electrons ( $N_e$ ) (dot-dash and dash curves respectively) are also shown.

the transition region, predicted to be a thin layer separating the chromosphere and corona in models, may also be quite different in reality.

The bulk of the electromagnetic radiation from the chromosphere and corona has much higher photon energies than those of visible-wavelength radiation, which range from 1.6 eV to 3 eV. The characteristic radiation emitted by material with temperatures of between 100 000 K and a few MK has photon energies between 10 eV and a few 100 eV, corresponding to wavelengths between  $\sim 1000$  Å and less than  $\sim 100$  Å. The solar chromosphere and corona are therefore strong emitters of radiation with wavelengths between the ultraviolet and soft X-ray range.

The high temperatures of the chromosphere and corona, much exceeding the photospheric temperature, are plainly departures from those expected from physical considerations. A heating mechanism, due to some non-radiant energy source, is therefore required. This energy source, as well as the structured nature of the chromosphere and corona, is strongly correlated with the Sun's magnetic field, a fact

that is readily observed: regions of the solar atmosphere hotter than their surroundings, as deduced from their ultraviolet and X-ray spectra, are highly correlated with regions in the photosphere associated with strong magnetic field.

Below the photosphere, interaction between the atoms or ions and the radiation that they emit is complete, and thermodynamic equilibrium occurs. Towards the solar surface, some of this radiation begins to escape to space, and thus becomes visible to instruments on Earth. Analysis of the spectrum of this radiation shows that there is a local thermodynamic equilibrium (LTE), in which the emitted radiation is characterized by local values of temperature and density. Farther out, there is an increasing departure from LTE, with the radiated energy from the photosphere interacting less and less with the surrounding material. Eventually, ions and electrons making up the hot corona, even though bathed in the strong photospheric radiation, are nearly unaffected by it.

The Sun is a second-generation star, formed by the coalescence of material left by first-generation stars in our Galaxy that underwent supernova explosions. This is reflected in the Sun's chemical composition, which is (by number of atoms) 90% hydrogen, nearly 10% helium, with trace amounts of heavier elements. In the chromosphere, with temperatures up to  $10^4$  K, the hydrogen is partially ionized, so that there are large numbers of free protons and electrons as well as neutral atoms of H and He. In the corona, the ionization of both hydrogen and helium is almost complete, so that the composition is free protons and electrons and He nuclei, with much smaller numbers of ions, including those of heavier elements. Thus, the corona is for many practical purposes a fully ionized plasma, having the associated properties that we discuss in Section 1.7.

### 1.3 The Ultraviolet and X-ray Spectrum of the Solar Atmosphere

The comparatively high temperatures and low densities of the solar atmosphere beyond the temperature minimum region result in a spectrum in the X-ray and ultraviolet ranges which at wavelengths less than  $\sim 1400$  Å is made up of emission lines and continuum. The lines and continua are due to specific ions or neutral atoms which we shall indicate by the appropriate element symbol and its degree of ionization. We use throughout this book a standard spectroscopic notation identifying the ionization degree with a Roman numeral; thus C I indicates the spectrum of neutral carbon (read as “the first spectrum of carbon”), C II indicates the spectrum of once-ionized carbon ions ( $C^+$ ) (“the second spectrum of carbon”), and so on. The ions themselves are indicated by superscripted numbers showing the numbers of electrons removed, e.g.  $C^{+3}$  indicates three-times-ionized carbon, which emits the C IV spectrum.

Figure 1.2 (upper panel) shows the ultraviolet disk spectrum of the quiet Sun in the range  $800 - 1500$  Å from the Solar Ultraviolet Measurements of the Emitted Radiation (SUMER) instrument on the *Solar and Heliospheric Observatory (SOHO)*. On the logarithmic flux scale of this figure, the most striking feature is the presence of recombination edges in the continuum spectrum. In the range included, these are at  $912$  Å (the Lyman continuum edge, due to the recombination of hydrogen),  $1100$  Å (recombination to neutral carbon, C I), and  $1197$  Å (S I). At longer wavelengths, there are edges at  $1527$  Å (Si I),  $1683$  Å (Si I),  $1700$  Å (Fe I), and  $1950$  Å

### 1.3 The Ultraviolet and X-ray Spectrum of the Solar Atmosphere 11

(Si I). Model atmosphere calculations, such as the Harvard Smithsonian Reference Atmosphere (Gingerich et al. (1971)) with subsequent corrections for line blanketing and absorption by molecules, give information about the location in the quiet Sun atmosphere where these continuum sources arise. Broadly, the continuum at wavelengths above the Si I edge at 1683 Å is emitted at photospheric layers, the region between the two Si I edges at 1527 Å and 1683 Å is emitted in the temperature minimum region, and the continuum shortward of 1527 Å is chromospheric in origin. Like the visible photospheric spectrum, spectroheliograms made in the ultraviolet continuum at  $\lambda > 1683$  Å show limb darkening. Immediately below this wavelength, and continuing into the X-ray range, spectroheliograms in the continuum emission show limb brightening.

To the long wavelength side of each recombination edge are members of line series that converge on each edge. Thus, members of the hydrogen Lyman line series converge on the Lyman continuum edge at 912 Å. The most prominent member of this series, and indeed the most intense (by two orders of magnitude) line of the entire solar ultraviolet spectrum, is the Ly- $\alpha$  line at 1215.67 Å. As this line can normally only be emitted in regions cool enough for neutral hydrogen to exist, its emission has its origins almost entirely in the chromosphere, though Ly- $\alpha$  emission by recombination and resonant scattering has been observed in the high-temperature corona (Gabriel et al. (1971)). The high abundance of hydrogen results in the line core being optically thick, and the line profile has a double reversal. There are two emission peaks separated by about 0.4 Å, with an absorption core which is formed high in the chromosphere, where the temperature is 40 000 K. The total width (FWHM) of the line is 0.7 Å, but the wings of the line, formed in the low chromosphere (temperature 6 000 K), extend out to about 15 Å either side of the line core. The amount of the absorption dips in the line profile centre varies according to the solar feature emitting the Ly- $\alpha$  line – see Figure 1.3, based on measurements of Fontenla et al. (1988). Actually, the Ly- $\alpha$  line is in theory a doublet through the interaction of the spin of the single electron in hydrogen with the orbital angular momentum of the electron, but the separation of the two components (0.0054 Å) is far less than the width of the solar line profile, which is determined by Doppler (thermal velocity) and Stark (pressure) mechanisms as well as instrumental broadening (this is about 0.01 Å for the measurements shown in Figure 1.3). Other prominent lines in the Lyman series include Ly- $\beta$  (1025.72 Å, also doubly reversed), Ly- $\gamma$  (972.54 Å), and Ly- $\delta$  (949.74 Å). Helium emission lines are also prominent, both those due to neutral (He I) and ionized (He II) atoms. Since ionized helium is like hydrogen but with a nuclear charge of +2 instead of +1 atomic units, its spectrum consists of a sequence of Lyman-like spectral lines but with wavelengths that are a factor 4 smaller than those of H. The Ly- $\alpha$  line of He II is thus a prominent line at 303.79 Å, formed in the transition region. Neutral helium lines have a rather more complex sequence, with lines at 584.31 Å, 537.01 Å, 522.19 Å etc., all chromospherically formed.

Thousands of other emission lines occur in the 800–1500 Å quiet Sun spectrum (Figure 1.2, upper panel), emitted in the chromosphere, transition region, and corona by ions of elements other than H or He. In the Appendix, we give a comprehensive list of these lines with wavelengths and identifications. The most intense emission lines are generally emitted by ions of abundant elements such as C, N, O, Ne, Mg, Si, S,

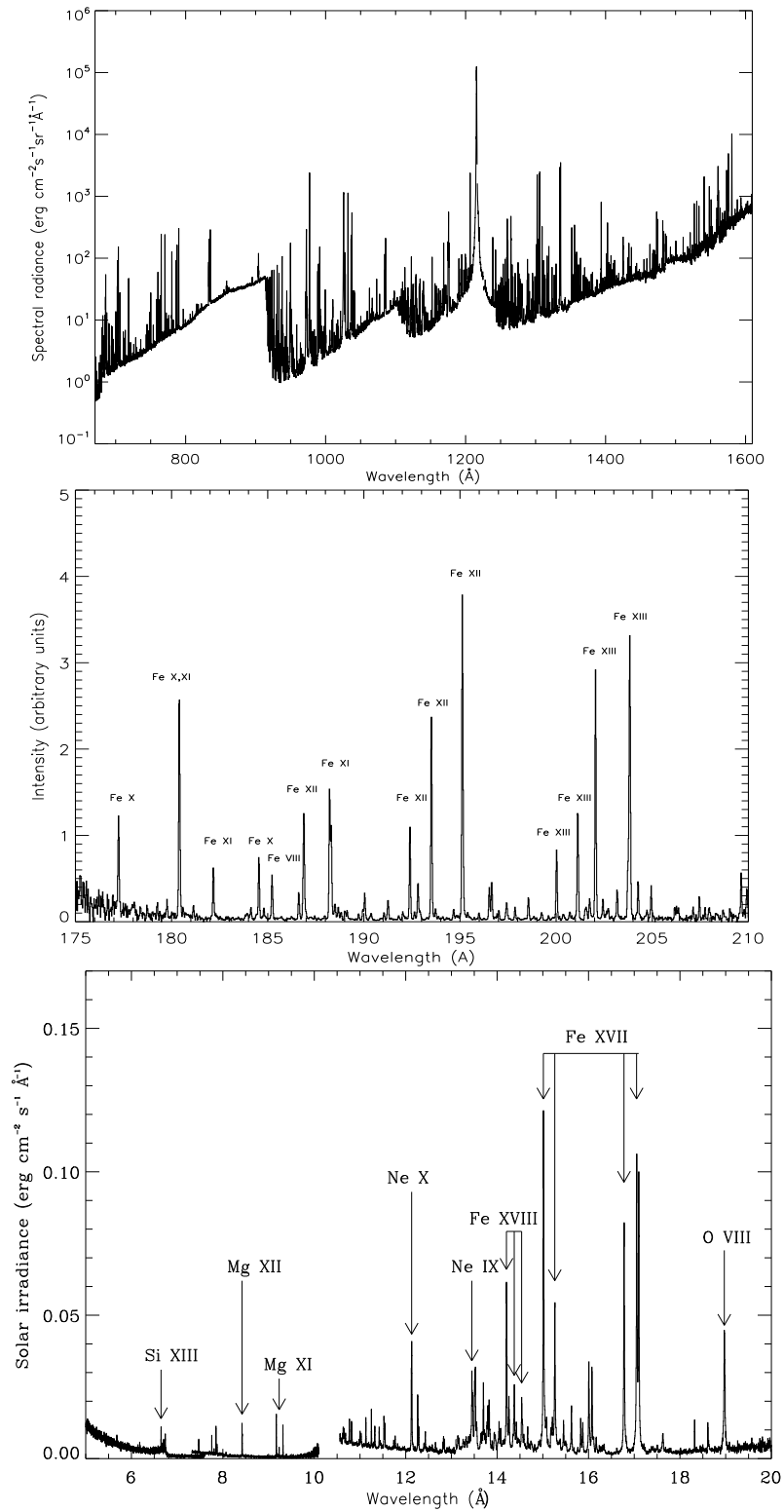


Fig. 1.2. Examples of solar ultraviolet, extreme ultraviolet, and X-ray spectra. (*Upper:*) *SOHO* SUMER quiet Sun disk spectrum in the 675–1600 Å range, showing the Lyman lines (particularly Ly- $\alpha$  line at 1215.67 Å), the Lyman recombination edge at 911.8 Å and the C I recombination edge at 1101.2 Å. (*Middle:*) Quiet Sun disk spectrum from the Extreme-ultraviolet Imaging Spectrometer (EIS) on the *Hinode* spacecraft, showing the diagnostically important lines of Fe ions between 175 Å and 210 Å, formed at coronal temperatures. Courtesy the *Hinode* EIS Team. (*Lower:*) Flare X-ray spectrum from the Flat Crystal Spectrometer on *Solar Maximum Mission*.